Charge-Transfer Salts of Octamethylferrocenyl Thioethers and $[M(mnt)_2]^-$ Complexes (M = Ni, Co, Pt). Synthesis, Structure, and Physical Properties

Stefan Zürcher, Volker Gramlich, Dieter von Arx, and Antonio Togni*

Laboratory of Inorganic Chemistry, ETH-Zentrum, Swiss Federal Institute of Technology, CH-8092 Zürich, Switzerland

Received February 24, 1998

The new ferrocene derivatives $Fe(\eta^5\text{-}C_5Me_4SR)_2$ (R = Me, **4**: R = *t*-Bu, **5**) have been prepared from the corresponding cyclopentadiene and $FeCl_2$. **5** may be converted to the bis(thiobenzoate) **6**, a protected form of dithiol **8**. From **6** the octamethyl trithiaferrocenophane **9** may be obtained in good yields. Compounds **4** and **5** are easily oxidized and form paramagnetic salts containing $[M(mnt)_2]^-$ anions (M = Co, Ni, Pt). The derivatives $[Fe(\eta^5\text{-}C_5Me_4SMe)_2][Ni(mnt)_2]$, **14**, $[Fe(\eta^5\text{-}C_5Me_4SMe)_2][Pt(mnt)_2]$, **15**, $[Fe(\eta^5\text{-}C_5Me_4SMe)_2][Co(mnt)_2]$, **16**, $[Fe(\eta^5\text{-}C_5Me_4S\textit{t}\text{-}Bu)_2][Ni(mnt)_2]$, **17**, $[Fe(\eta^5\text{-}C_5Me_4S\textit{t}\text{-}Bu)_2][Pt(mnt)_2]$, **18**, and $[Fe(\eta^5\text{-}C_5Me_4S\textit{t}\text{-}Bu)_2][Co(mnt)_2]$, **19**, have been prepared and fully characterized. X-ray crystal structural studies of **14** and **16**−**19** have been carried out. **14** and **16** display stacks of strongly interacting $[M(mnt)_2]^-$ anions, whereas **19** contains discrete $[Co(mnt)_2]$ dimers. **17** and **18** are isomorphous and display a typical $D^+A^-D^+A^-$ structural motif. SQUID susceptibility measurements indicate a weak ferromagnetic ordering at low temperature for these two compounds.

Introduction

Decamethylferrocene has been used since almost two decades as an electron donor for the formation of charge-transfer (CT) complexes with a variety of electron acceptors.[1] The radical cation/radical anion salts thus formed display a wide range of magnetic behaviors, from, e.g., metamagnetism for $[FeCp^*_2][TCNQ]$,[2] to bulk ferromagnetism for the corresponding CT complex containing tetracyanoethylene reported by Miller and co-workers.[3] Beside these systems containing organic acceptors, analogous CT complexes formed from inorganic acceptors such as monoanionic maleonitrilodithiolate metal complexes ($M(mnt)_2$) have been reported.[4]

We note that the tridimensional solid-state structure of such CT complexes is both very much unpredictable and of primary importance in determining the magnetic properties. Similarly, the packing of anions and cations is a very significant issue also in the related field of organic superconductors.[5] Thus, an alternation between the acceptor and the compact, highly symmetrical (C_{5v}) decamethylferrocene seems to be one necessary condition for magnetic cooperativity.[4a] With these considerations in mind, we previously described studies concerning the use of new, less symmetrical (C_2, C_s) ferrocene derivatives containing conjugated sulfur heterocycles and demonstrated their ability to form, e.g., semiconducting CT complexes.[6] In continuation of these studies, we report herein the synthesis of new 1,1′-bis(alkylthio)octamethylferrocenes of C_{2v} or C_{2h} symmetry. These compounds turn out to be excellent electron donors affording highly crystalline CT complexes with $M(mnt)_2$ acceptors, partly displaying the structural requirements for magnetic cooperativity.

Results and Discussion

Synthesis and Properties of Sulfur Substituted Octamethylferrocenes. We first attempted to prepare octamethylferrocene bis(thioethers) by alkylation of the corresponding dithiol. However, whereas ferrocene 1,1′-dithiol is accessible in two steps from ferrocene (dilithiation followed by the reaction with elemental sulfur and reduction), a similar procedure fails in the octamethyl series. An alternative route was found involving the reaction of the known 1-bromo-2,3,4,5-tetramethylcyclopentadiene[7] (**1**) with thiolates and subsequent formation of the

(1) For reviews, see: (a) Togni, A. In *Ferrocenes. Homogeneous Catalysis, Organic Synthesis, Materials Science*, Togni, A., Hayashi, T., Eds.; VCH: Weinheim, 1995; pp 433−469. (b) Epstein, A. J.; Miller, J. S. *Angew. Chem.* **1994**, *106*, 399−432 (*Angew. Chem., Int. Ed. Engl.* **1994**, *33*, 385−416) and references therein. For selected original papers, see: (c) Gebert, E.; Reis, A. H.; Miller, J. S.; Rommelmann, H.; Epstein, A. *J. Am. Chem. Soc.* **1982**, *104*, 4403−4410. (d) Broderick, W. E.; Thompson, J. A.; Godfrey, M. R.; Sabat, M.; Hoffman, B. M. *J. Am. Chem. Soc.* **1989**, *111*, 7656−7657. (e) Eichhorn, D. M.; Skee, D. C.; Broderick, W. E.; Hoffmann, B. M. *Inorg. Chem.* **1993**, *32*, 491−492. (f) Broderick, W. E.; Hoffmann, B. M. *J. Am. Chem. Soc.* **1991**, *113*, 6334−6335. (g) Broderick, W. E.; Thompson, J. A.; Day, E. P.; Hoffmann, B. M. *Science* **1990**, *249*, 401−403.

(2) Reis, A. H.; Preston, L. D.; Williams, J. M.; Peterson, S. W.; Candela, G. A.; Swartzendruber, L. J.; Miller, J. S. *J. Am. Chem. Soc.* **1979**, *101*, 2755−2758.

(3) (a) Miller, J. S.; Calabrese, J. C.; Epstein, A. J.; Bigelow, R. W.; Zhang, J. H.; Reiff, W. M. *J. Chem. Soc., Chem. Commun.* **1986**, 1026−1028. (b) Miller, J. S.; Epstein, A. J.; Reiff, W. M. *Science* **1988**, *240*, 40−47.

(4) a) Miller, J. S.; Calabrese, J. C.; Epstein, A. J. *Inorg. Chem.* **1989**, *28*, 4230−4238. (b) Fettouhi, M.; Ouahab, L.; Hagiwara, M.; Codjovi, E.; Kahn, O.; Constant-Machado, H.; Varret, F. *Inorg. Chem.* **1995**, *34*, 4152−4159.

(5) For a discussion of structural aspects in organic superconductors, see, e.g.: Williams, J. M.; Ferraro, J. R.; Thorn, R. J.; Carlson, K. D.; Geiser, U.; Wang, H. H.; Kini, A. M.; Whangbo, M.-H. *Organic Superconductors (Including Fullerenes). Synthesis, Structure, Properties, and Theory*; Prentice Hall: Englewood Cliffs, NJ, 1992; Chapter 3, pp 65−114.

(6) (a) Togni, A.; Hobi, M.; Rihs, G.; Rist, G.; Albinati, A.; Zanello, P.; Zech, D.; Keller, H. *Organometallics* **1994**, *13*, 1224−1234. (b) Hobi, M.; Zürcher, S.; Gramlich, V.; Burckhardt, U.; Mensing, C.; Spahr, M.; Togni, A. *Organometallics* **1996**, *15*, 5342−5346. (c) Hobi, M.; Ruppert, O.; Gramlich, V.; Togni, A. *Organometallics* **1997**, *16*, 1384−1391.

(7) Jutzi, P.; Schwartzen, K.; Mix, A. *Chem. Ber.* **1990**, *123*, 837−840.

S0020-1669(98)00204-3 CCC: $15.00
Published on Web 07/23/1998

Scheme 1

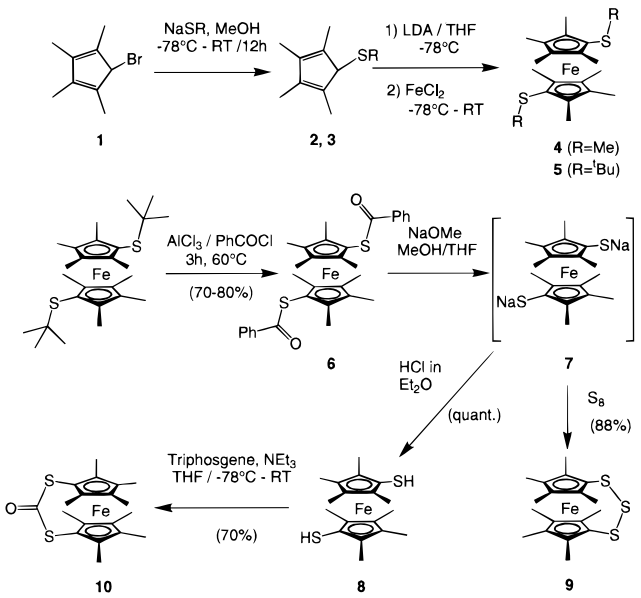

ferrocenes, as shown in Scheme 1. Thus, the thermally labile tetramethylthioalkylcyclopentadienes **2** and **3** were obtained in good yields as mixtures of isomers, differing in the position of the diene system with respect to the position of the sulfur substituent (only one isomer is shown in Scheme 1). Deprotonation with LDA and reaction with anhydrous $FeCl_2$ in THF afforded the ferrocenes **4** and **5** in moderate to good yields. The *tert*-butyl thioether **5** was converted in the presence of $AlCl_3$ to the corresponding bis(thiobenzoate) **6**, a protected form of dithiol **8**. The latter was prepared and isolated as a very air-sensitive material upon methanolysis to the reactive disodium dithiolate **7** (not isolated) and protonation in diethyl ether. Furthermore, reaction of **7** with sulfur gave the octamethyl trithiaferrocenophane **9** in good yield. Finally, the carbonyl ferrocenophane **10** was obtained from the dithiol upon reaction with triphosgene in the presence of NEt_3. The preparations of compounds **6**−**10** is reported here to illustrate the synthetic utility of thioethers **4** and **5**. However, their chemistry, in particular involving CT complexes of ferrocenophane **9**, shall be described elsewhere.

Routine cyclovoltammetric measurements, carried out in dichloromethane show a totally reversible (as indicated by the ratio of i_{pc} and i_{pa} of 1.0) one electron oxidation step at −0.23 V for **4** and −0.25 V for **5**, as referred to the ferrocene/ferrocenium couple. This is ca. 0.25 V higher, as compared to decamethylferrocene. Yet higher redox potentials are displayed by derivatives **6**, **9**, and **10** in which the two sulfur substituents fully counter balance the eight methyl groups in determining the redox propensity. For comparison, analogous measurements have been carried out for the $[M(mnt)_2]$ salts under identical conditions.[8] Redox potentials are reported in Table 1.

(8) Redox potentials of $[M(mnt)_2]^-$ derivatives in different solvents and referred to different standard electrodes have been reported previously. See: a) McCleverty, J. A. *Prog. Inorg. Chem.* **1968**, *10*, 50−215. (b) Nüsslein, F.; Kisch, H.; Peter, R. *Chem. Ber.* **1989**, *122*, 1023−1030. (c) Schmauch, G.; Knoch, F.; Kisch, H. *Chem. Ber.* **1994**, *127*, 287. (d) Holm, R. H.; Davison, A. *Inorg. Synth.* **1967**, *10*, 8−26. (e) Gama, V.; Henriques, R. T.; Bonfait, G.; Almeida, M.; Meetsma, A.; van Smaalen, S.; de Boer, J. L. *J. Am. Chem. Soc.* **1992**, *114*, 1986−1989. (f) Gama, V.; Henriques, R. T.; Almeida, M.; Veiros, L.; Calhorda, M. J.; Meetsma, A.; Boer, J. L. *Inorg. Chem.* **1993**, *32*, 3705−3711. For a discussion of the redox couple Fc/Fc^+, see: Conelly, N. G.; Geiger, W. E. *Chem. Rev.* **1996**, *96*, 877−910.

Table 1. Formal Electrode Potentials (vs Fc/Fc^+) for Ferrocene and $M(mnt)_2$ Derivatives in Dichloromethane Solution[a]

compound (reduced form)	$E_1^{\circ\prime}$ [V]	ΔE_p [mV]	i_{pc}/i_{pa}	$E_2^{\circ\prime}$ [V]	ΔE_p [mV]	i_{pc}/i_{pa}	$E_3^{\circ\prime}$ [V]
$Fe(\eta^5\text{-}C_5Me_5)_2$	−0.48	110					
$Fe(\eta^5\text{-}C_5Me_4SCMe_3)_2$	−0.29	134	1.00				
$Fe(\eta^5\text{-}C_5Me_4SMe)_2$	−0.27	218	1.00				
$Fe(\eta^5\text{-}C_5Me_4SCOPh)_2$	−0.09	98	0.98				
$Fe(\eta^5\text{-}C_5Me_4S)_2CO$	+0.08	120	1.01				
$Fe(\eta^5\text{-}C_5Me_4S)_2S$	−0.10	272	1.00				
$[Ni(mnt)_2]^-$	−0.31	266	0.94	+0.69	144	0.69	
$[Pt(mnt)_2]^-$	−0.32	86	0.96	+0.59	103	0.84	
$[Co(mnt)_2]^-$	−0.51	164	1.06	+0.34[b]	116	0.92	(+0.98)

[a] All experiments carried out in dry dichloromethane/0.1 M $[NBu_4]BF_4$ vs 0.05 M Fc/Fc^+ reference electrode with $E^{\circ\prime} = +0.042$ V for ferrocene, and a Pt working electrode (all values are corrected for 0 V). Values in brackets are E_{pa} (anodic peak potential) only assigned to irreversible oxidation steps. Scan rate: 100mV/s. [b] $[Co(mnt)_2]_2^{2-}/[Co(mnt)_2]_2^-$ (values of i_{pc} and i_{pa} are exactly half compared to the first oxidation step).

Scheme 2

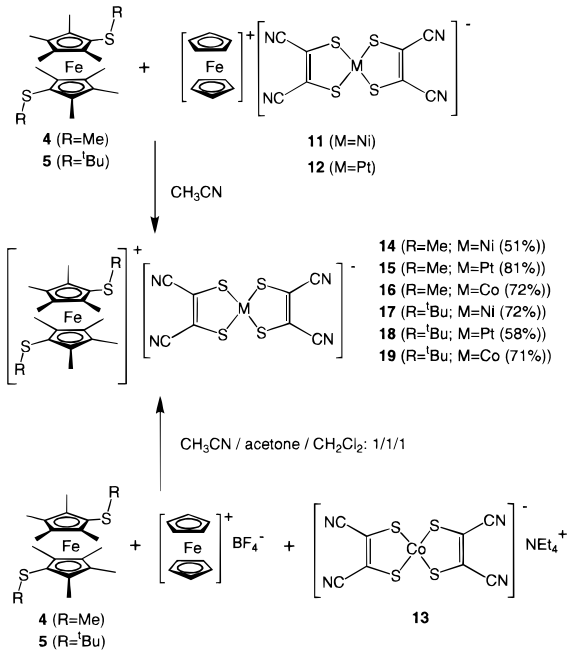

Synthesis of Charge-Transfer Complexes. For the synthesis of CT complexes containing the monoanionic, formally M(III) acceptors $[M(mnt)_2]^-$ (M = Ni, Pt, Co) and the ferrocene donors **4** and **5**, two different strategies were used. For the nickel and platinum derivatives, the reagents $[FeCp_2]^+[M(mnt)_2]^-$ were the key intermediates fulfilling two functions: (1) delivering the anion $[M(mnt)_2]^-$ and (2) oxidizing the desired donor, the only byproduct being the readily soluble ferrocene. The ferrocenium salts **11** and **12** were obtained as previously reported from our laboratory.[6b] Their reaction with the donors **4** and **5**, respectively, in hot acetonitrile gave after evaporation of the solvent the desired CT complexes that were purified by recrystallization from ethyl acetate and obtained as shiny black crystals in moderate to good yields, as shown in Scheme 2. For the cobalt analogues, probably because of the different redox behavior and the pronounced tendency to dimerize, we were not able to prepare $[FeCp_2]^+[Co(mnt)_2]^-$. Therefore, the donors were first oxidized with $[FeCp_2]^+BF_4^-$ and then added to $(NEt_4)^+[Co(mnt)_2]^-$ [9] to obtain the desired products **16** and **19** in good yields. For all CT complexes **14**−**19** a clean 1:1

Table 2. Experimental Data for the X-ray Diffraction Studies of **14**, **16**, **17**, **18** and **19**

	14	**16**	**17**	**18**	**19**
empirical formula	$C_{28}H_{30}N_4S_6FeNi$	$C_{28}H_{30}CoFeN_4S_6$	$C_{34}H_{42}N_4S_6FeNi$	$C_{34}H_{42}N_4S_6FePt$	$C_{34}H_{42}N_4S_6FeCo$
mol wt	729.5	729.70	813.6	950.0	813.9
crystal dimens, mm	0.2 × 0.25 × 0.4	0.2 × 0.4 × 0.4	0.2 × 0.38 × 0.4	0.6 × 0.6 × 0.9	0.2 × 0.4 × 0.4
cryst syst	triclinic	monoclinic	triclinic	triclinic	triclinic
space group	$P\bar{1}$ (No. 2)	$P2(1)/n$ (No. 14)	$P\bar{1}$ (No. 2)	$P\bar{1}$ (No. 2)	$P\bar{1}$ (No. 2)
temp	room temp	room temp	room temp	room temp	room temp
a (Å)	8.649(3)	15.109(10)	9.619(9)	9.591(4)	10.007(5)
b (Å)	14.080(4)	8.588(6)	9.622(10)	9.681(3)	14.481(7)
c (Å)	15.358(4)	25.36(20)	11.253(12)	11.252(2)	15.024(7)
α_(deg)	65.27(2)	90.00	79.72(9)	78.17(2)	104.79(2)
β_(deg)	77.77(2)	99.12(6)	78.66(8)	78.47(3)	97.21(2)
γ_(deg)	80.78(2)	90.00	76.62(8)	77.38(3)	107.47(2)
V (Å$^{3)}$	1654.8(9)	3248.9(40)	984(2)	984.6(5)	1959(2)
Z	2	4	1	1	2
ρ (calcd) (g cm^{-3})	1.464	1.492	1.373	1.602	1.380
μ (cm^{-1})	14.11	13.68	67.45	42.63	94.94
diffractometer	Syntex P21	Syntex P21	Picker-Stoe	Syntex P21	Picker-Stoe
radiation	Mo Kα, λ = 0.710 73 Å	Mo Kα, λ = 0.710 73 Å	Cu Kα, λ = 1.541 78 Å	Mo Kα, λ = 0.710 73 Å	Cu Kα, λ = 1.541 78 Å
θ range (deg)	1.60−20.04	1.63−20.04	4.05−49.99	1.87−20.04	3.12−50.00
no. of measd reflcns	3362	3150	2023	1812	4013
no. of indep data collcd	3091	3053	2023	1812	4013
no. of obsd reflcns (n)[a]	2614	2523	1768	1778	3065
no. of params refined (p)	362	362	212	233	419
wR2 [$I > 2\sigma(I)$][b]	0.1293	0.1245	0.1479	0.1006	0.1240
R1 [$I > 2\sigma(I)$][c]	0.0467	0.0406	0.0597	0.0386	0.0505
GOF[d]	1.051	1.044	1.052	1.071	1.070

[a] ($|F_o^2| > 4.0\ \sigma(|F|^2)$). [b] $wR2 = [\sigma[w(F_o^2 - F_c^2)^2]/\sigma[w(F_o^2)^2]]^{1/2}$. [c] $R1 = \sigma||F_o| - |F_c||/\sigma|F_o|$. [d] $GOF = S = [\sigma\ (w(F_o^2 - F_c^2)^2]/(n - p)]^{1/2}$.

stoichiometry of donor and acceptor was observed in product crystals, even when the precursors were mixed in different ratios.

For $[M(mnt)_2]$ derivatives the CN stretching frequency of the mnt ligand provides a diagnostic tool correlating with the state of charge of the whole fragment. All new $[M(mnt)_2]$ compounds of this study display sharp ν(CN) bands in the narrow range between 2205 and 2209 cm^{-1}. This is also true for the starting monoanionic forms $[NEt_4][M(mnt)_2]$ (2205−2208 cm^{-1}).

Solid-State Structure of Charge-Transfer Salts. For the 1:1 salts obtained above and containing charge-transfer partners differing only in the nature of the thioalkyl substituent on the ferrocene unit or having a different metal in the anionic counterpart, respectively, it was of interest to observe how such relatively small variations would influence the solid-state structure. Crystals suitable for X-ray diffraction studies were obtained for compounds **14** and **16**−**19**. Table 2 gives the relevant crystal and data collection parameters. Bond distances and angles of each asymmetric unit were found to fall in the expected ranges and will not be discussed here (they are provided as Supporting Information, along with ORTEP representations). Figures 1−4 illustrate the relative arrangement of the molecular components of each compound in tridimensional space.

In the structure of **14** pairs of ferrocenium cations (Fe−Fe distance 9.90 Å) form columns, each of which is surrounded by four stacks of $[Ni(mnt)_2]$ anions, as shown by the projection along the crystallographic *a* axis of Figure 1. No inversion center coincides with either the nickel or iron atom. This leads to C_1 symmetry for the ferrocenium ion. The two Cp rings are almost ideally parallel, with an interplanar angle of 2°, and are rotated with respect to each other by 86° along the molecular vertical axis. The $[Ni(mnt)_2]$ units form dimers with the Ni atom interacting with a sulfur atom of the second fragment at a distance of 3.72 Å. This leads to a zigzag arrangement along the Ni stacks with alternating Ni−Ni distances of 4.29 and 5.10 Å.[6b,10] In the asymmetric unit the plane of the anion is very much tilted with respect to the plane of the Cp ring close to it, the corresponding interplanar angle being 78°.

The general qualitative structural features of the analogous Co compound **16** (see Figure 2) are very similar to those of **14**, with the same relationships between $[Co(mnt)_2]$ stacks and ferrocenium columns. However, the $[Co(mnt)_2]$ units form, as expected, much tighter centrosymmetric dimers, with a pronounced pyramidalization of the Co centers.[4b] Along the Co stacking direction (crystallographic *b* axis) the difference between the alternating long and short metal−metal distances is also more conspicuous than in the Ni derivative (3.15 and 5.47 Å, respectively). The ferrocenium cation shows an almost antiperiplanar conformation, with the two Cp rings being rotated 169° with respect to each other.

The two Ni and Pt compounds **17** and **18**, respectively, both containing the bulkier ferrocenium cation derived from **5**, are isomorphous. The most prominent general structural feature of these compounds is constituted by the presence of alternating layers of $[M(mnt)_2]$ and ferrocenium units. The Ni and Pt atoms, respectively, occupy the corners of the unit cell, whereas the Fe centers are located in the center of each *bc* plane, thus corresponding to an inversion center. Along the crystallographic (0 1 1) and (0 1−1) vectors a $D^+A^-D^+A^-$ structural motif with two different Fe−Ni distances of 6.72 and 8.03 Å is apparent (in the Pt compound the corresponding distances are 6.63 and 8.14 Å), as shown in Figure 3. The Fe−Fe distances and M−M distances (Ni−Ni and Pt−Pt) correspond to the unit cell dimensions. Along the *b* axis, two $[M(mnt)_2]$-units are separated by two *tert*-butyl groups of two adjacent ferrocenium ions. The angle between the Cp plane and the plane of the $[M(mnt)_2]$ anion in the asymmetric unit is 46° in **17** and 44° in **18**, respectively. The latter planes are also tilted with respect to the *bc* plane, i.e., for the anion by ca. 20°, thus recalling a scaled structure, and by ca. 35° for the ferrocenium. Finally, the sulfur atoms

(9) (a) Edelstein, N.; Holm, R. H.; Maki, A. H.; Davison, A. *Inorg. Chem.* **1963**, *2*, 1227. (b) Holm, R. H.; Davison, A. *Inorg. Synth.* **1967**, *10*, 8−26. (c) Bray, J.; Locke, J.; McCleverty, J. A.; Coucouvanis, D. *Inorg. Synth.* **1971**, *13*, 187−195.

(10) Weiher, J. F.; Melby, L. R.; Benson, R. E. *J. Am. Chem. Soc.* **1964**, *86*, 4329−4333.

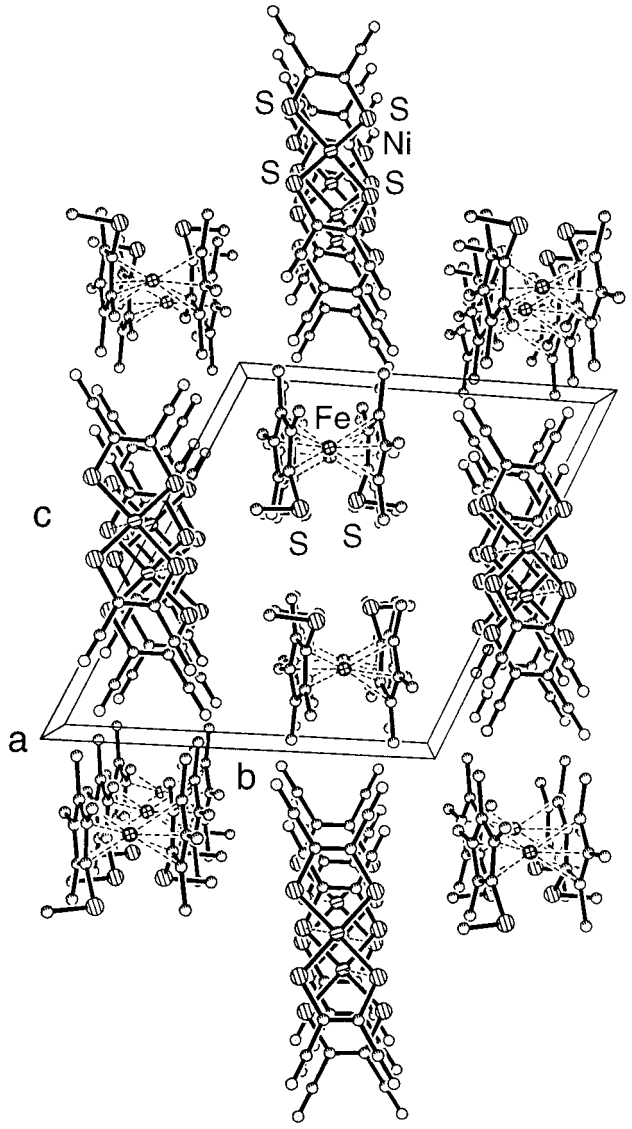

Figure 1. Perspective view of $[Fe(\eta^5\text{-}C_5Me_4SMe)_2][Ni(mnt)_2]$, **14**, down the crystallographic *a* axis, showing the four stacks of $[Ni(mnt)_2]$ anions surrounding a double column of ferrocenium cations.

are located at 0.08 Å (**17**) and at 0.10 Å (**18**) below the respective Cp plane, i.e., in the region between the two Cp rings.

For the last member of the series, compound **19**, differing from its companions **17**-**18** only by the replacement of Ni/Pt by Co, yet a different structure is observed. As shown in Figure 4, the presence of $[Co(mnt)_2]^-$ dimers leads to a structure best described as belonging to the $D^+(A_2)^{2-}D^+$ type. The iron atoms of the two inequivalent ferrocenium cations in the unit cell coincide with two symmetry centers, one in the middle of the *a* axis, the other at the center of the *bc* plane. The $[Co(mnt)_2]_2$ dimeric unit is centrosymmetric and resides in the middle of the *c* axis.

Magnetic Measurements. Magnetic susceptibility measurements were carried out for the CT complexes **14**−**19** using a SQUID susceptometer in the temperature range between 2 and 300 K. Plots of the reciprocal susceptibility $1/\chi_{mol}$ and of $\chi_{mol}T$ vs T, respectively, are shown in Figure 5. The compounds **14**−**19** obey a modified Curie−Weiss expression $\chi = C/(T + \theta) + q$, where q is the sum of core diamagnetism and temperature independent paramagnetism (TIP). For all compounds q is positive, meaning that TIP is larger than the diamagnetic component.

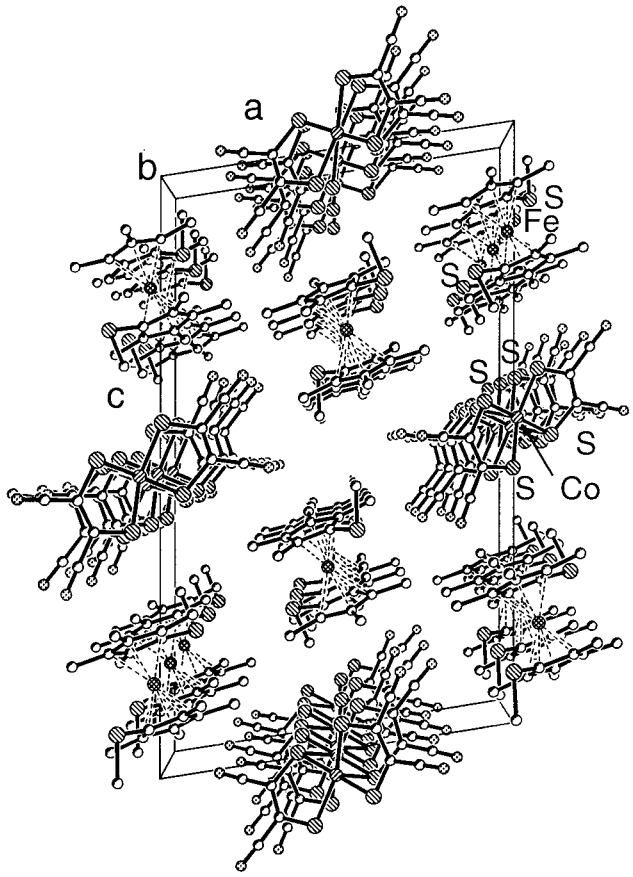

Figure 2. Perspective view of $[Fe(\eta^5\text{-}C_5Me_4SMe)_2][Co(mnt)_2]$, **16**, down the crystallographic *b* axis.

For compounds **14**−**16** and **19** , θ values of zero (**16**, **19**) or slightly negative (**14**, **15**) were found. For **14** and **15** this observation, together with the abrupt drop of $\chi_{mol}T$ at temperatures below 50 K, indicates a transition most likely dominated by intermolecular antiferromagnetic interactions. However, alternatively to such a magnetic ordering, this behavior could be explained by a depopulation of spin−orbit states. From the high temperature $\chi_{mol}T$ data the effective magnetic moments may be calculated ($\mu_{eff} = (3k\chi_{mol}T/N\beta^2)^{1/2}$). They assume values between 1.73 μ_B/mol for **16** and 2.73 μ_B/mol for **15**. Thus, the former case turns out to be a perfect $S = {}^1/_2$ system with non interacting spins. This behavior may be well understood on the basis of the solid-state structure discussed above. The $[Co(mnt)_2]^-$ units form diamagnetic stacked dimers and the magnetic properties are conveyed by the virtually isolated ferrocenium ions.

A significantly different magnetic behavior is shown by the two derivatives **17** and **18**. In fact, an increase of $\chi_{mol}T$ in the low-temperature range, as well as a positive θ value of ca. 3 K for both compounds is observed (also the effective magnetic moment is 2.68 μ_B/mol for **17** and 2.94 μ_B/mol for **18**). This is indicative of a weak but significant ferromagnetic coupling. This magnetic ordering becomes possible because of the alternating $D^+A^-D^+A^-$ structure common to these two compounds (see above),[4a] impeding strong interactions between $[M(mnt)_2]^-$ units.

Conclusions

We have shown that new persubstituted ferrocene derivatives suited as electron donors and containing thioethers fragments are easily accessible from the corresponding preformed cyclo-

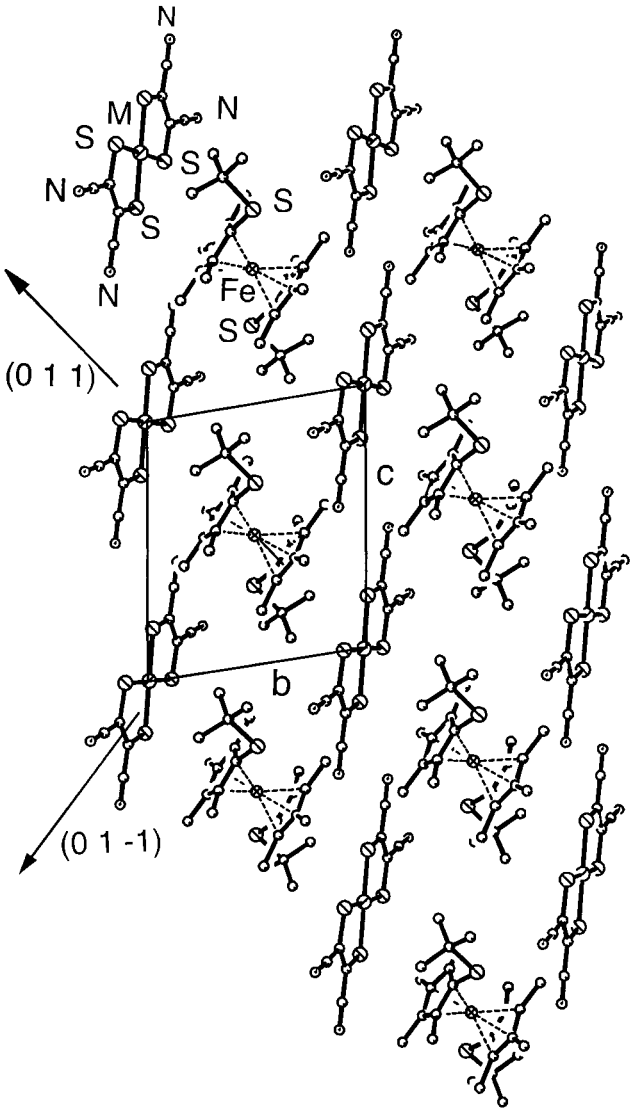

Figure 3. Perspective view of the two isomorphous compounds [Fe(η^5-C_5Me_4St-Bu)$_2$][M(mnt)$_2$] (M = Ni, **17**; M = Pt, **18**) down the crystallographic *a* axis, showing the typical alternating $D^+A^-D^+A^-$ arrangement.

pentadienes. These donors, in their oxidized form, lead to crystalline salts with $[M(mnt)_2]^-$ derivatives. Subtle and nonpredictable changes in the solid state structure are observed upon changing the nature of the alkyl group on sulfur. Whereas methyl derivatives give structures containing stacked and strongly interacting anions, their *tert*-butyl counterparts favor alternating arrangements of donors and acceptors in the solid state, with a typical $D^+A^-D^+A^-$ structure for the isomorphous compounds **17** and **18**. The structural differences are in turn responsible for the different magnetic behaviors observed, a weak ferromagnetic coupling arising from the alternating framework.

We are currently studying the properties of analogous compounds derived from donors **4** and **5** and containing electron acceptors derived from the TCNQ basic structure. The results of these studies shall be reported in due course.

Experimental Section

General experimental techniques were described earlier.[6a]

2,2′,3,3′,4,4′,5,5′-Octamethyl-1,1′-bis(methylthio)ferrocene (4). 2,3,4,5,-Tetramethyl-1-methylthiocyclopentadiene (**2**): 8.6 g (70 mmol) of tetramethylcyclopentadiene was dissolved in 250 mL of hexane and cooled to 0 °C. A 44 mL (70 mmol) amount of a 1.6 M *n*-BuLi solution in hexane was added. The resulting mixture was stirred and allowed to warm to room temperature overnight. A solution of 7.4 g (70 mmol) of cyanogen bromide in 20 mL of diethyl ether was then added over a period of 30 min at −78 °C. The mixture was stirred for 2h at −78 °C and then warmed slowly to 0 °C. The yellow solution was filtered, and the solvents were evaporated. The resulting yellow 1-bromo-2,3,4,5-tetramethylcyclopentadiene (**1**) was directly dissolved in 150 mL of MeOH and cooled to −78 °C. A 5.0 g (71 mmol) amount of NaSMe was added, and the mixture was allowed to warm to room temperature overnight. The solvent was removed under vacuum, and the desired product was extracted with hexane. Yield: 10.8 g (92%) of a yellow oil. This product proved to be a mixture of several isomers of 1-methylthio-2,3,4,5-tetramethylcyclopentadiene (**2**) (by NMR) and was used without further purification. MS: *m*/*z* 168 (M^+, 100), 153, 139, 120, 105, 91, 79.

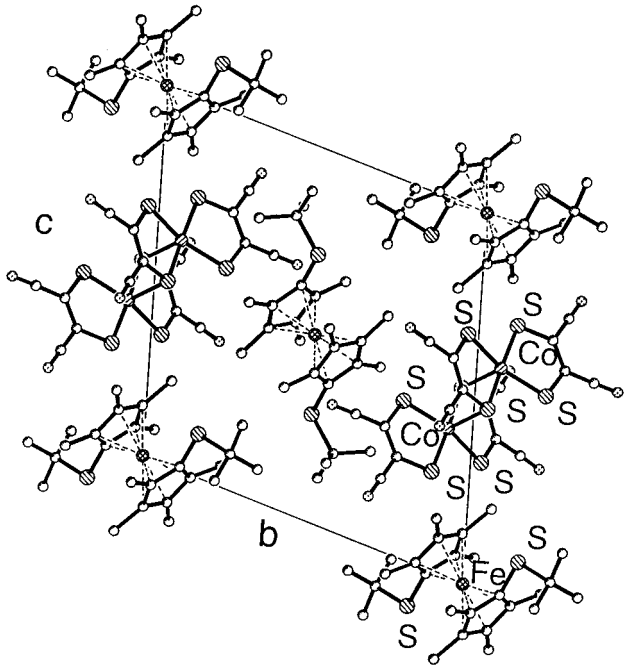

Figure 4. Perspective view of [Fe(η^5-C_5Me_4St-Bu)$_2$][Co(mnt)$_2$], **19**, down the crystallographic *a* axis, showing the [Co(mnt)$_2$] dimers.

The intermediate thioether (**2**) thus obtained (10.8 g, 57.5 mmol) was dissolved in 100 mL of THF, cooled to −78 °C, and mixed with a freshly prepared solution of lithium diisopropylamide (from 9.8 mL of diisopropylamine, 45.8 mL of 1.6 M of *n*-BuLi, and 50 mL of THF). The mixture was stirred for 10 min, and then 6.1 g (48.18 mmol) of $FeCl_2$ was added in small portions. The mixture was allowed to warm to room temperature overnight and was then refluxed for an additional hour. The black reaction mixture was mixed with dichloromethane and extracted twice with 2 N HCl and sodium dithionite and once with water. The organic layer was evaporated and flash chromatographed with hexane/EtOAc, v/v 20:1. Yield: 4.97 g (40% from tetramethylcyclopentadiene). Mp: 152−154 °C (dec). ^{1}H NMR (250.13 MHZ, $CDCl_3$): δ 1.76 (s, 12H), 1.87 (s, 12H), 1.99 (s, 6H). ^{13}C NMR (62.895 MHZ, $CDCl_3$): δ 9.34, 18.49, 77.99, 81.20, 83.60. MS: *m*/*z* 390 (M^+, 100), 375, 344, 327, 297, 254, 223, 205, 195, 174, 151, 119, 105, 91, 56. Anal. Calcd for $C_{20}H_{30}S_2Fe$: C, 61.53; H, 7.74; S, 16.43. Found: C, 61.58; H, 7.90; S, 16.65. IR (KBr): 2967, 2914, 1448, 1419, 1372, 1360, 1332.

2,2′,3,3′,4,4′,5,5′-Octamethyl-1,1′-bis(*tert*-butylthio)ferrocene (5). 2,3,4,5,-Tetramethyl-1-(*tert*-butylthio)cyclopentadiene (**3**) was obtained in an analogous manner as described above for the methylthio derivative from 6.58 g (53.8 mmol) of tetramethylcyclopentadiene, 250 mL of hexane, 27 mL (53.8 mmol) of 2.0 M *n*-BuLi in hexane, 5.69 g (53.8 mmol) of cyanogen bromide in 20 mL of diethyl ether, and 6.45 g (57.5 mmol) of NaS*t*-Bu in 150 mL of MeOH, yielding 8.3 g (57.5 mmol, 73%) of the crude mixture of isomers (MS: *m*/*z* 210 (M^+), 154 (100), 139, 120, 105, 91, 77, 57). After dissolution in 100 mL of THF,

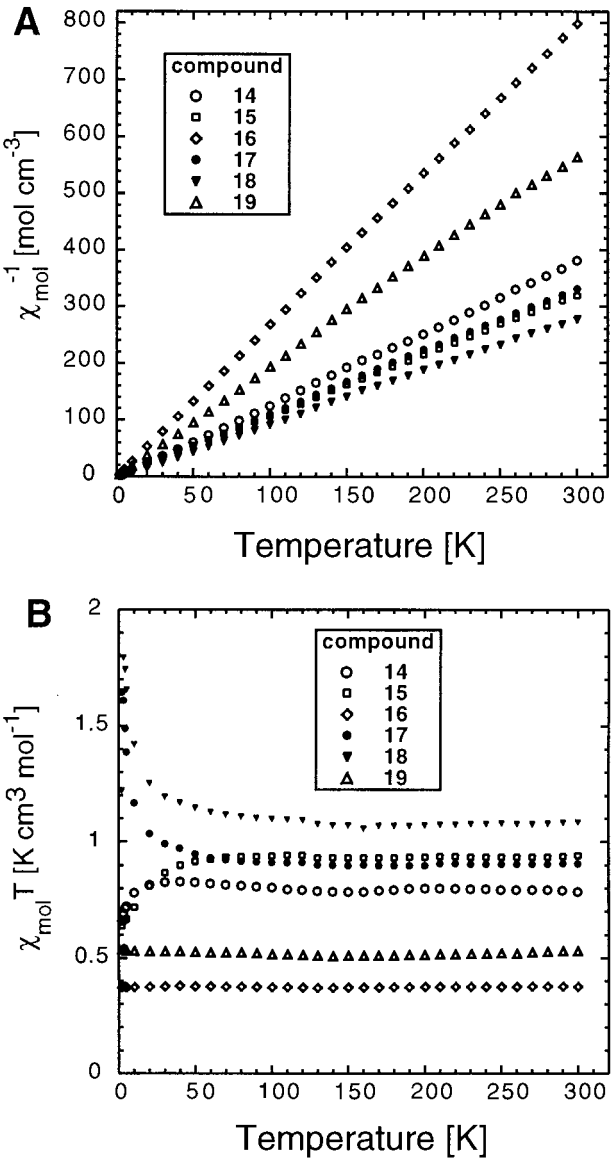

Figure 5. SQUID susceptibility data for compounds **14**-**19** measured in an external magnetic field of 1000 G.

the ligand was treated with a freshly prepared solution of lithium diisopropylamide (from 8.3 mL of diisopropylamine, 28.1 mL of 1.6 M *n*-BuLi in hexane, and 50 mL of THF) and subsequently with 3.75 g (29.6 mmol) of $FeCl_2$, as described above. Yield: 7.29 g (57% from tetramethylcyclopentadiene). Mp: 179 °C (dec). ^{1}H NMR (250.13 MHZ, $CDCl_3$): δ 1.13 (s, 18H), 1.76 (s, 12H), 1.85 (s, 12H). ^{13}C NMR (62.895 MHZ, $CDCl_3$): δ 9.91, 11.16, 31.26, 46.36, 75.40, 82.01, 84.61. MS: *m*/*z* 474 (M^+, 100), 418, 362, 327, 294, 206, 174, 119, 105, 57. Anal. Calcd for $C_{26}H_{42}S_2Fe$: C, 65.80; H, 8.92; S, 13.51. Found: C, 65.86; H, 8.78; S, 13.24. IR (KBr): 2960, 2898, 1472, 1457, 1375, 1360, 1323, 1170, 1025, 992, 518, 466, 451.

2,2′,3,3′,4,4′,5,5′-Octamethylferrocen-1,1′-diyl Bis(thiobenzoate) (6). A 3 g (6.3 mmol) amount of **5** and 1.8 g (12.6 mmol) of $AlCl_3$ were suspended in 20 mL of benzoyl chloride. The reaction mixture was heated to 60 °C for 3 h, and then the excess of benzoyl chloride was removed under reduced pressure. The residue was dissolved in CH_2Cl_2/MTBE and extracted twice with saturated $NaHCO_3$ solution and once with lime. The organic phase was dried with $MgSO_4$ and evaporated, and the residue was chromatographed over silica (hexane/toluene 1/5). The product was recrystallized from CH_2Cl_2/hexane to yield 2.86 g (79%) of a yellow powder. Mp: 242 °C (dec). ^{1}H NMR: δ 1.79 (s, 12H), 1.85 (s, 12H), 7.4−7.7 (m complex, 8H), 8.0−8.1 (m complex, 2H). ^{13}C NMR (62.895 MHz): δ 9.74, 9.82, 69.88, 82.86, 84.41, 127.43, 128.59, 133.30, 136.84, 129.19. MS: *m*/*z* 570 (M^+, 100), 556, 490, 465, 434, 360, 329, 313, 285, 209, 174, 119, 105, 77. Anal. Calcd for $C_{32}H_{34}O_2S_2Fe$: C, 67.36; H, 6.01; S 11.24. Found: C, 67.45; H 5.97; S, 11.37. IR (KBr): 2968, 2905, 1675, 1579, 1446, 1377, 1310, 1206, 1170, 1028, 1001, 902, 771, 685, 645, 616, 554, 509, 467, 445.

2,2′,3,3′,4,4′,5,5′-Octamethyl-ferrocene-1,1′-dithiol (8). A 200 mg (0.35 mmol) amount of **6** and 123 mg (2.2 mmol) of NaOMe were dissolved in 30 mL of THF/MeOH (1:1) and stirred overnight at room temperature. To this solution was added 2.2 mL of 1.0 M HCl solution (2.2 mmol) in Et_2O, and the solvents were evaporated. Extraction with Et_2O (or MTBE) yielded the dithiol **8** in quantitative yield. ^{1}H NMR (250.13 MHz, $CDCl_3$): δ 1.71 (s, 12H), 1.93 (s, 12H). ^{13}C NMR (62.895 MHz, $CDCl_3$): δ 9.30, 9.85, 80.70, 83.13. MS: *m*/*z* 362 (M^+, 100), 329, 295, 241, 209. Anal. Calcd for $C_{18}H_{26}S_2Fe$: C, 59.66; H, 7.23; S, 17.70. Found: C, 59.77; H7.02; S, 17.49. IR (KBr): 2968, 2944, 2903, 2512 (S−H st), 1637, 1461, 1374, 1028, 455.

2,2′,3,3′,4,4′,5,5′-Octamethyl-1,1′-trithia[3]ferrocenophane (9). The disodium bisthiolate **7** was prepared in situ from 1.152 g (2 mmol) of **6** and 648 mg (12 mmol) of NaOMe as described above. A 512 mg (16 mmol) amount of sulfur was added, and the resulting suspension was stirred for 24 h. The solvents were evaporated, and the residue was chromatographed over silica with hexane as eluent. Yield: 644 mg (81%). ^{1}H NMR (250.13 MHz, $CDCl_3$): δ 1.35 (s, 6H), 1.49 (s, 6H), 1.63 (s, 6H), 1.67 (s, 6H). ^{13}C NMR (62.895 MHz, $CDCl_3$): δ 8.196 (2*CH_3), 8.698 (4*CH_3), 9.784 (2*CH_3), 78.548, 81.175, 82.994, 87.142, 89.180. MS: *m*/*z* 392 (M^+, 100), 359, 325, 240, 206, 152, 119, 91, 56. Anal. Calcd for $C_{18}H_{24}S_3Fe$: C, 55.09; H, 6.16; S, 24.51. Found: C, 55.33; H, 5.97; S, 24.20. IR (KBr): 2970, 2947, 2902, 1474, 1451, 1375, 1320, 1153, 1027, 746, 616, 513, 488, 462, 389, 376.

2,2′,3,3′,4,4′,5,5′-Octamethyl-1,1′-dithiacarbonyl[3]ferrocenophane (10). A 317 mg (0.87 mmol) amount of **8** was dissolved in 20 mL of THF and cooled to −78 °C. Triphosgene (86.5 mg, 0.29 mmol) was added, and 242 μL (1.74 mmol) of NEt_3 was added dropwise to the resulting solution. The reaction mixture was allowed to warm to room temperature, and the solvent was evaporated. Chromatographic purification of the residue over silica (hexane/toluene 5:2) yielded 236 mg (70%) of the product. ^{1}H NMR (250.13 MHz, $CDCl_3$): δ 1.50 (s, 12H), 1.71 (s, 12H). ^{13}C NMR (62.895 MHz, $CDCl_3$): δ 9.496, 9.646, 74.531, 84.529, 84.573. MS: *m*/*z* 388 (M^+), 360, 327(100), 294, 205, 174, 119, 91, 56. Anal. Calcd for $C_{19}H_{24}OS_2Fe$: C, 58.76; H, 6.23; S, 16.51. Found: C, 58.71; H, 6.23; S, 16.54. IR (KBr): 3199, 2906, 1612, 1458, 1378, 1030, 894, 470, 430.

[$FeCp_2$][$Pt(mnt)_2$] (12). A 1.00 g (0.959 mmol) amount of $[NBu_4]_2[Pt(mnt)_2]$ and 0.57 g (2.0 mmol) of $[FeCp_2]BF_4$ were separately dissolved in 1,2-dichloroethane (50 and 100 mL, respectively). The ferrocinium solution was filtered and slowly added dropwise to the solution of $[NBu_4]_2[Pt(mnt)_2]$. Diethyl ether (100 mL) was added, and the green microcrystalline material which formed was filtered off. Yield: 466 mg (73%). Mp: >260 °C (dec). Anal. Calcd for $C_{18}H_{10}N_4S_4FePt$: C, 32.68; H, 1.52; N, 8.47. Found: C, 32.66; H, 1.74; N, 8.31. IR (KBr): 3106, 2207, 1442, 1414, 1162, 1108, 1057, 1006, 850, 519, 500.

Preparation of Charge-Transfer Complexes. The procedure for the preparation of CT complexes with $[M(mnt)_2]^-$ (M = Ni, Pt, Co) is exemplified by the synthesis of **14**. **4** (100 mg, 0.256 mmol) and $[FeCp_2][Ni(mnt)_2]$ (135 mg, 0.256 mmol) were dissolved in hot acetonitrile, filtered, and dried in vacuo. The brown-black residue was recrystallized from EtOAc to obtain small shiny black crystals. Yield: 96 mg (51%). Mp: 199 °C (dec). Anal. Calcd for $C_{28}H_{30}N_4S_6FeNi$: C, 46.10; H, 4.14; N, 7.68. Found: C, 46.20; H, 4.00; N, 7.73. IR (KBr): 2980, 2926, 2207, 1450, 1378, 1307, 1159, 1026, 970, 524, 500.

Compound **15** was obtained in an analogous manner from 100 mg (0.256 mmol) of **4** and 169 mg (0.256 mmol) of $[FeCp_2][Pt(mnt)_2]$. Yield: 180 mg (81%). Mp: 214 °C (dec). Anal. Calcd for $C_{28}H_{30}N_4S_6FePt$: C, 38.84; H, 3.49; N, 6.47. Found: C, 38.81; H, 3.47; N, 6.44. IR (KBr): 2980, 2926, 2209, 1458, 1439, 1379, 1162, 1017, 698, 668, 524, 499.

Compound **16** was obtained similarly from 100 mg (0.256 mmol) of **4**, 70 mg (0.256 mmol) of $[FeCp_2]BF_4$ in acetone/CH_2Cl_2 (1/1), and 120 mg (0.256 mmol) of $[Co(mnt)_2]NEt_4$ in hot acetonitrile. Yield:

150 mg (72%). Mp: >260 °C (dec). Anal. Calcd for $C_{28}H_{30}N_4S_6FeCo$: C, 46.09; H, 4.14; N, 7.68. Found: C, 45.99; H, 4.32; N, 7.62. IR (KBr) 2924, 2205, 1453, 1379, 1309, 1157, 1025, 968, 696, 570, 508, 467.

Compound **17** was obtained similarly from 50 mg (0.105 mmol) of **5** and 55.1 mg (0.105 mmol) of $[FeCp_2][Ni(mnt)_2]$. Yield: 61.5 mg (72%). Mp: 210 °C (dec). Anal. Calcd for $C_{34}H_{42}N_4S_6FeNi$: C, 50.19; H, 5.20; N, 6.89. Found: C, 50.15; H, 5.12; N, 6.89. IR (KBr): 2959, 2208, 1473, 1454, 1381, 1363, 1160, 1025, 570, 526, 502.

Compound **18** was obtained similarly from 93.3 mg (0.196 mmol) of **5** and 130.2 mg (0.196 mmol) of $[FeCp_2][Pt(mnt)_2]$. Yield: 107 mg (58%). Mp: 224 °C (dec). Anal. Calcd for $C_{34}H_{42}N_4S_6FePt$: C, 42.98; H, 4.46; N 5.90. Found: C, 42.90; H, 4.24; N, 6.04. IR (KBr): 2976, 2959, 2922, 2209, 1473, 1458, 1441, 1382, 1366, 1162, 1025, 668, 571, 500.

Compound **19** was obtained similarly from 100 mg (0.21 mmol) of **5**, 98.6 mg (0.21 mmol) of $[Co(mnt)_2]NEt_4$, and 57.2 mg (0.21 mmol) of $[FeCp_2]BF_4$. Yield: 120 mg (70.5%). Mp: 240 °C (dec). Anal. Calcd for $C_{34}H_{42}N_4S_6FeCo$: C, 50.17; H, 5.20; N, 6.88. Found: C, 50.37; H, 5.13; N, 6.91. IR (KBr): 2960, 2920, 2896, 2862, 2205, 1473, 1456, 1380, 1364, 1160, 1025, 572, 528, 508.

X-ray Crystallographic Study of 14, 16, 17, 18, and 19. Suitable crystals for an X-ray analysis of all these compounds were obtained by slow diffusion of hexane into a solution of the CT complex in dichloromethane. Selected crystallographic and relevant data collection parameters are listed in Table 2. Data were measured at room temperature with variable scan speed to ensure constant statistical precision on the collected intensities. One standard reflection was measured every 120 reflections and no significant variation was detected. The structures were solved by Patterson Methods and refined by full-matrix least-squares using anisotropic displacement parameters for all non hydrogen atoms. The contribution of the hydrogen atoms in their idealized position (Riding model with fixed isotropic $U = 0.080$ Å^2) was taken into account but not refined. All calculations were carried out by using the Siemens SHELX93 (VMS) system.

Magnetic Measurements. The magnetic susceptibility χ of CT complexes **14**−**19** was measured in the temperature range of 2−300 K in an external variable magnetic field, by means of a Quantum Design superconducting quantum interference device (SQUID) magnetometer. The polycrystalline samples were mounted in a sample holder tube made of quartz glass in order to keep the magnetic background as low as possible. Routine corrections for core diamagnetism, temperature independent paramagnetism and the sample holder were applied.

Acknowledgment. S.Z. is grateful to the Swiss National Science Fundation for financial support (Grant No. 20-41974.94).

Supporting Information Available: Tables of atomic coordinates, complete listing of bond distances and angles, tables of anisotropic displacement coefficients, coordinates of hydrogen atoms, as well as ORTEP representations and atom numbering schemes for **14** and **16**−**19** (39 pages). Ordering and access information is given on any current masthead page. Tables of calculated and observed structure factors may be obtained from the authors upon request.

IC9802045